



Titel

Advances in detector development  
for Muon Spin Spectroscopy

Ersetzt

Autoren /  
Autorinnen

A. Stoykov, R. Scheuermann

Erstellt

22.02.2009

**Zusammenfassung:**

Recent rapid progress in the development of Geiger-mode Avalanche PhotoDiodes (G-APDs) triggered an "avalanche" of applications of this novel photodetector, especially in such fields as high energy physics and nuclear medicine. In this work we review advances in application of G-APDs in Muon Spin Spectroscopy.

Verteiler	Abt.	Empfänger / Empfängerinnen	Expl.	Abt.	Empfänger / Empfängerinnen	Expl.		Expl.
	3501	A. Amato	1				Bibliothek	3
	3000	R. Bercher	3				Reserve	3
	3000	K. Clausen	1				Total	16
	8580	K. Deiters	1				Seiten	14
	3500	E. Morenzoni	1				Beilagen	
	3502	T. Prokscha	1				Informationsliste	
	1412	D. Renker	1				D 1 2 3 4 5 8 9 A	
	1414	N. Schlumpf	1				Visum Abt.-/Laborleitung:	
							<i>E. Morenzoni</i>	



# Introduction

Throughout the history of the  $\mu$ SR experimental technique [1] a photomultiplier tube (PMT) detecting light from plastic scintillators is an indispensable part of any  $\mu$ SR spectrometer. The presence of external magnetic fields applied in a  $\mu$ SR experiment necessitates using light guides to deliver the scintillation light to PMTs. Such an approach works well for the “standard” spectrometers that do not use highly segmented detectors and in moderate (up to 1 Tesla) fields. Increasing the detector segmentation and/or going to higher (up to 10 Tesla) magnetic fields will make the use of PMTs more problematic due to the space limitations and the degradation of the time resolution caused by attenuation and broadening of the light pulses in the light guides.

To create the basis for further development of the  $\mu$ SR technique, in 2003 at the Swiss Muon Source ( $S\mu S$ ) [2] of the Paul Scherrer Institut (PSI, Villigen, Switzerland) we started developing magnetic field insensitive scintillation detectors based on Geiger-mode Avalanche Photodiodes (G-APDs) [3]. This work summarizes our up-to-date achievements in this field.

## 1 G-APD – a solid-state photomultiplier

The G-APD is a solid-state photodetector realized as a matrix of tiny, virtually independent Avalanche PhotoDiodes (called pixels or cells): all of them are connected to a common load and biased above the breakdown voltage (see Fig. 1). When a free charge carrier is created (either by a photon, or is generated thermally) in the active volume of a cell, it triggers an avalanche breakdown in this particular cell. As a result, the voltage on the cell drops to the breakdown value and a current pulse appears in the load circuit. The charge in this pulse is equal to the charge stored in the pixel capacitance. The gain of the G-APD is this charge divided by the unit charge. When several cells are firing at the same time, for example in response to a light pulse, their signals are summed.

Different types of G-APDs are now produced by a variety of companies and research groups throughout the world, each producer giving the device a new name. This fact is somewhat confusing especially for a novice in the field. One should keep in mind that such names as Silicon PhotoMultiplier (SiPM), Avalanche Microchannel PhotoDiode (AMPD), Micropixel Avalanche Photodiode (MAPD), Metal-Resistive layer Silicon Avalanche PhotoDiode (MRS APD), Solid State PhotoMultiplier (SSPM), MultiPixel Photon Counter (MPPC), multipixel Geiger-mode Avalanche PhotoDiode (G-APD) are all referring to photodetectors based on the same operation principle described above (although some of them might differ significantly in realization). The name G-APD, proposed in [3], is not related to any producer and will be used in this paper to refer to any device of this family. When discussing some particular device we will use the name given by its producer.

When choosing a G-APD for some particular application, one has to consider the following parameters: 1) active area:  $1 - 25 \text{ mm}^2$ ; 2) number of cells:  $100 - 40000 \text{ mm}^{-2}$ ; 3) photon detection efficiency; 4) gain:  $10^4 - 10^7$ ; 5) single-photon time resolution; 6) excess noise; 7) inter-pixel cross-talk; 8) operating voltage:  $15 - 150 \text{ V}$ ; 9) dark current:  $0.01 - 10 \text{ }\mu\text{A}/\text{mm}^2$  at RT; 10) dark counts:  $0.1 - 10 \text{ MHz}/\text{mm}^2$  at RT; 11) cell recovery time:  $5 - 10000 \text{ ns}$ ; 12) temperature coefficient of gain:  $0.1 - 10 \text{ \%}/\text{K}$ ; 13) radiation hardness.

Among the numerous research papers contributing to understanding the performance of G-APDs and to the method of measuring their parameters we can highlight the following: a) review papers [3, 4, 5, 6]; b) dynamic range and non-linearity effects [7, 8]; c) photon detection efficiency and excess noise [9]; d) recovery time [10, 11]; e) radiation

hardness [12].

Compared to PMTs, G-APDs have the following advantages: they are insensitive to magnetic fields, they are compact and robust, and they require low operation voltage. Accordingly, G-APDs are well suited for compact, finely segmented detectors and detectors to be used in a high magnetic field environment. A disadvantage of G-APDs is their comparatively small active area (a larger area photosensor can be built by combining together several G-APDs as has been shown in [13]).

## 2 Experience with G-APDs in $\mu$ SR instrumentation

Development of G-APD based scintillation detectors at  $S\mu$ S of PSI has been going in three directions: 1) position sensitive detectors for muon beam profile measurements; 2) “large” area detectors (tens of square cm) with “standard” time resolution ( $\sigma < 400$  ps); 3) compact fast-timing detectors with  $\sigma < 100$  ps.

### 2.1 A scintillating fiber muon beam profile monitor

Beam profile measurements are essential for the setup of  $\mu$ SR instruments. A Muon Beam Profile Monitor ( $\mu$ BPM) [14], see Fig. 2, was designed to measure the profile of a “surface” ( $\sim 28$  MeV/c) muon beam inside the warm bore of a 5 Tesla superconducting solenoid of the Avoided Level Crossing (ALC) spectrometer [2]. The device consists of 10 + 10 scintillating fibers spaced along X and Y directions. The fibers are readout by AMPDs developed in Dubna (Russia). Each AMPD is mounted on a separate amplifier board.

The  $\mu$ BPM probes the beam intensity profile at the positions of the fibers, i.e it simultaneously measures two one-dimensional X and Y distributions. By using the  $\mu$ BPM an oscillatory behavior of the muon beam spot size as a function of the magnetic field created by the solenoid was measured (see Fig. 3). Later the effect was reproduced in GEANT-4 simulations [15].

Further development of such type of detector would include implementing the real two-dimensional capabilities (i.e probing the beam intensity profile at the fiber intersection points by counting coincidence rates between the X and Y channels instead of their individual rates) and extending the detection capabilities to muons with higher momentum (and respectively with lower energy losses).

### 2.2 ALC spectrometer – first $\mu$ SR instrument dispensing with photomultiplier tubes

A well-known approach to build large area scintillation counters is a so-called tile-fiber detector, where the light from a scintillating tile is collected to a photosensor by means of wavelength shifting (WLS) fibers [16, 17, 18]. This technology is mainly used when very large areas (starting from square meters) have to be covered with scintillation detectors, the design of the detector often being a trade-off between the price and the performance.

In [13] we demonstrated a possibility to build a high-performance tile-fiber detector suitable for  $\mu$ SR applications. Relying on this experience, in [19] we undertake the task of building a new detector system for the 5 Tesla ALC instrument.

The basic part of the ALC spectrometer is a superconducting solenoid with a room-temperature bore of 20 cm in diameter and a length of 1 m, which creates a longitudinal (with respect to the initial muon spin polarization) magnetic field up to 5 Tesla at its center. The detector module mounted in the bore of the solenoid is shown in Fig. 4. The

muons stop in the sample located at the center of the solenoid. The decay positrons emitted in the backward (BW) and forward (FW) directions with respect to the initial muon momentum are detected by two annular sets of scintillation counters. The spectrometer is operated in time-integral mode: for each value of the applied magnetic field the integral number of counts in BW and FW detector sets is recorded within a predefined time interval and then used to calculate the muon decay asymmetry. Time-differential mode of operation, i.e measurement of the correlations between muon implantation time and its decay time, is also possible by replacing one of the positron counters by a counter to detect incoming muons, see Fig. 5.

The BW (FW) positron counter, see Fig. 6, is based on an EJ-204 (ELJEN Technology) scintillator tile of dimensions  $120 \times 33 \times 5 \text{ mm}^3$  ( $120 \times 28 \times 5 \text{ mm}^3$ ). Two  $\varnothing 1 \text{ mm}$  WLS fibers type BCF-92 (Saint-Gobain Crystals) are glued into the grooves in the tile using BC-600 optical epoxy. The light emitted in the scintillator is collected by the fibers, re-emitted and subsequently transported to the photosensors – a pair of G-APDs connected in series. Additional amplification of the detector signal is done by an amplifier (gain  $\sim 20$ , bandwidth  $\sim 70 \text{ MHz}$ ) mounted inside the detector module. The G-APDs are of type SSPM-0701BG produced by Photonique SA [20]. The main criteria for choosing this G-APD were its high photon detection efficiency ( $PDE \approx 30\%$  at  $490 \text{ nm}$ ) as well as the very weak temperature dependence of the gain (temperature coefficient  $< 0.7\%/K$ ). The operating bias voltage for the pair of G-APDs is about  $40 \text{ V}$ .

Typical positron detection signals are shown in Fig. 7. At zero magnetic field the signals have a well-defined amplitude band, with the most probable pulse height value at  $\sim 350 \text{ mV}$ . This is about 90 times the pulse height of the 1-cell signals (the signals from the breakdown of single G-APD cells) and 12 times the minimum threshold required to suppress the noise from the thermally generated charge carries to less than 100 counts per second. The most probable charge of the positron signals corresponds to  $\sim 130$  simultaneously firing cells. As the magnetic field increases, higher amplitudes start to appear in the signal spectrum: positrons, now moving along helical trajectories, travel longer paths and therefore deposit more energy in the counters. The amplitude of the 1-cell signals at  $4.5 \text{ T}$  is about the same (within  $10\%$ ) as that at zero magnetic field (see Fig. 7) implying that neither the G-APD nor the amplifier gain are noticeably influenced by the field.

Due to a finite recovery time of the G-APD the counter signals decrease in amplitude with increasing rate. However, in normal operating conditions with positron rates below  $200 \text{ kHz}$  per counter this change of the amplitude is less than  $10\%$  (i.e., the pulse height is still well above the threshold level).

Figure 8 shows an example of the time-integral (ALC) data taken on a test sample. One full field range scan with a coarse step and one short range scan over the resonance at  $\mu_0 H \approx 2 \text{ T}$  using finer steps are reported. Note the exact reproducibility of the asymmetry baseline in the two scans indicating the high overall stability of the detector.

Figure 9 shows a time-differential spectrum taken on a silver sample in zero magnetic field. Notice very low level of the background  $B/N_0 = 2 \cdot 10^{-4}$  resulting from the chosen configuration of the detector. Although designed and optimized for TI-mode, the time resolution in TD-mode is in the sub-ns range characteristic for “standard”  $\mu\text{SR}$  spectrometers.

### 2.3 A challenge of Muon Spin Rotation experiments in 10 Tesla

Time-differential  $\mu\text{SR}$  relies on measuring correlations between the muon implantation and decay times. The accuracy of this measurement defines the capability of the spectrometer

to detect high frequency muon spin precession signals according to [21]:

$$a(\nu)/a_0 = \exp \left[ - \frac{(\pi 2.355 \sigma \nu)^2}{4 \ln 2} \right], \quad (1)$$

where  $a(\nu)$  is the amplitude of the precession signal of frequency  $\nu$  measured with time resolution  $\sigma$  (standard deviation);  $a_0$  is the maximum signal amplitude at  $\sigma = 0$ . Figure 10 shows the dependence of the measured signal amplitude on its frequency calculated using Eq. (1) for different values of  $\sigma$ . As is seen, in 10 Tesla a time resolution better than 140 ps is required in order to detect muon-spin precession with a Larmor frequency of 1.35 GHz (the measured amplitude is then above 50 % of the maximum value).

Realization of such fast-timing detectors in a traditional way, i.e by using photomultiplier tubes, is problematic due to the high magnetic field environment. PMTs, whose performance is strongly affected by the field, have to be placed in a low field region ( $\ll 1$  T) rather far from the scintillators, the scintillation light would be delivered to them by long light guides. The attenuation and broadening of the light pulses in the light guides lead to degradation of the time resolution. The only presently existing high field  $\mu$ SR spectrometer is the 7 T *HiTime* instrument at TRIUMF (Vancouver, Canada), which is equipped with a PMT-based detector system and has a time resolution of  $\sim 170$  ps [22].

The feasibility of muon spin rotation experiments in 10 Tesla has been proven in [23], where a setup with a time resolution of 65 ps in 4.8 T field was demonstrated. The construction of the used prototype counters and their response to muons and positrons are shown in Fig. 11 and 12, respectively. In addition to the excellent time resolution and insensitivity to the magnetic field the counters are capable to handle high event rates (see Fig. 13), which makes them suitable also for spectrometers at high intensity pulsed muon beams.

## Summary

In five years of R&D work in the field of application of G-APDs we demonstrated a large potential of these novel photodetectors for the development of the  $\mu$ SR technique. Research in this field has also been recently started in other  $\mu$ SR laboratories [24]. We are confident that G-APDs in the future will play the same role in  $\mu$ SR as PMTs have done for more than 40 years.

## Acknowledgments

We thank X. Donath, M. Elender, U. Greuter, Th. Proksha, D. Renker, R. Schmidt, K. Sedlak, T. Shiroka (PSI), K. Gritsay, Z. Sadygov, V. Zhuk (JINR), Yu. Musienko (CERN) contributed to this research project. We appreciate efforts of such companies as Dubna-Detectors Ltd., Photonique SA, Hamamatsu Photonics, and Zecotek in the development of G-APDs.

This work was fully performed at the Swiss Muon Source ( $S\mu S$ ) at the Paul Scherrer Institut in Villigen, Switzerland. The project has been partially supported by the European Commission under the 6th Framework Programme through the Key Action: Strengthening the European Research Area, Research Infrastructures. Contract no.: RII3-CT-2003-505925.

## References

- [1] The abbreviation  $\mu$ SR stands for Muon Spin Rotation / Relaxation / Resonance. A description of this experimental method in condensed matter research can be found in: A. Schenck, *Muon Spin Rotation Spectroscopy*, Adam Hilger Ltd., London, 1985.
- [2] <http://lmw.web.psi.ch>
- [3] D. Renker, Nucl. Instr. and Meth. A 567 (2006) 48.
- [4] B. Dolgoshein et al., Nucl. Instr. and Meth. A 563 (2006) 368.
- [5] Z. Sadygov et al., Nucl. Instr. and Meth. A 567 (2006) 70.
- [6] Y. Musienko et al., Nucl. Instr. and Meth. A 598 (2009) 213.
- [7] P. Buzhan et al., ICFA Instr. Bull. 23 (2001) 28.
- [8] A. Stoykov et al., Journal of Instrumentation JINST 2 (2007) P06005.
- [9] Y. Musienko et al., Nucl. Instr. and Meth. A 567 (2006) 57.
- [10] I. Britvitch, D. Renker, Nucl. Instr. and Meth. A 567 (2006) 260.
- [11] H. Oide et al., PoS (PD07) 008.
- [12] Y. Musienko et al., Nucl. Instr. and Meth. A 581 (2007) 433.
- [13] R. Scheuermann et al., Nucl. Instr. and Meth. A 581 (2007) 443.
- [14] A. Stoykov et al., Nucl. Instr. and Meth. A 550 (2005) 212.
- [15] T. Lancaster et al., Nucl. Instr. and Meth. A 580 (2007) 1578.
- [16] A.P. Ivashkin et al., Nucl. Instr. and Meth. A 394 (1997) 321.
- [17] A. Artikov et al., Particles and Nuclei, Letters 3/3 (2006) 81.
- [18] A. Akindinov et al., Nucl. Instr. and Meth. A 567 (2006) 74.
- [19] A. Stoykov et al., Physica B (in press);  
<http://dx.doi.org/10.1016/j.physb.2008.11.211>  
A. Stoykov et al., PSI Technical Report TM-35-08-01 (2008) 1-19.
- [20] <http://www.photonique.ch>
- [21] E. Holzschuh, Phys. Rev. B 27 (1983) 102.
- [22] S. Kreitzman, private communications.
- [23] A. Stoykov et al., Physica B (in press);  
<http://dx.doi.org/10.1016/j.physb.2008.11.210>
- [24] S. Takeshita et al., Nucl. Instr. and Meth. A 600 (2009) 139.

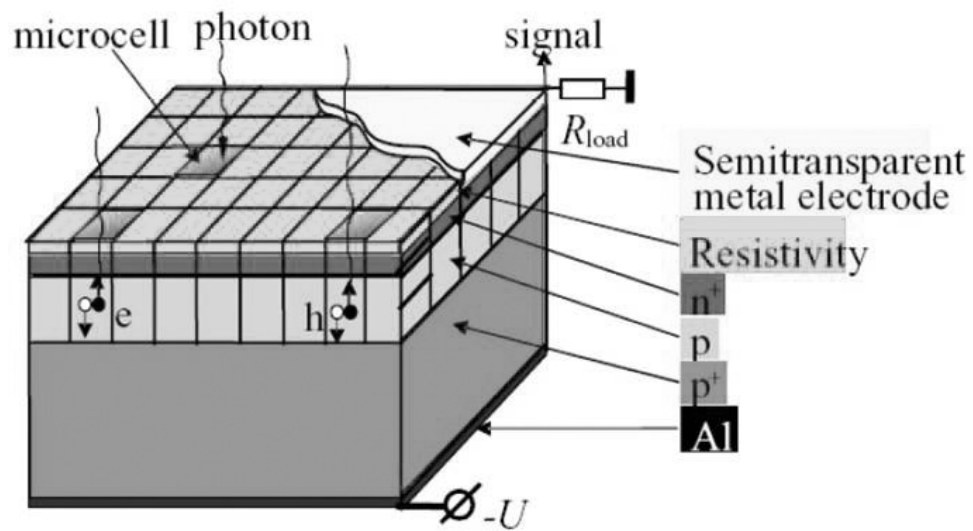


Figure 1: Illustration to the construction of a G-APD (picture is taken from the presentation given by A. Akindinov at the NDIP2005 conference).



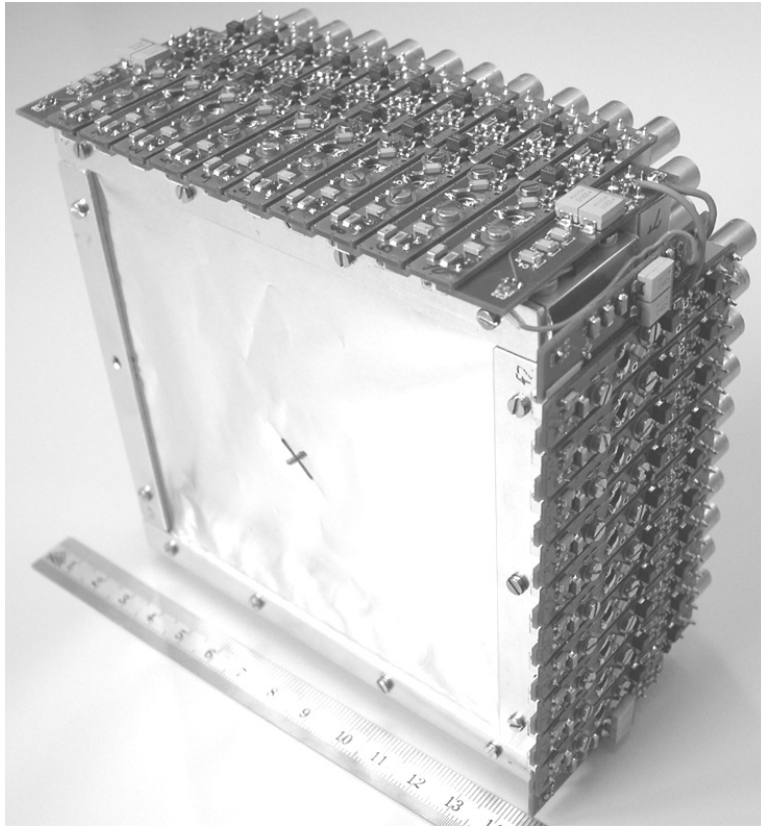


Figure 2:  $\mu$ BPM – a scintillating fiber detector for muon beam profile measurements in high magnetic fields. The device consists of 10 + 10 scintillating fibers spaced along two perpendicular directions (the fibers can not be seen because of aluminium foils used for light protection). For the readout of the fibers avalanche microchannel photodiodes are used, each mounted on a separate amplifier board.

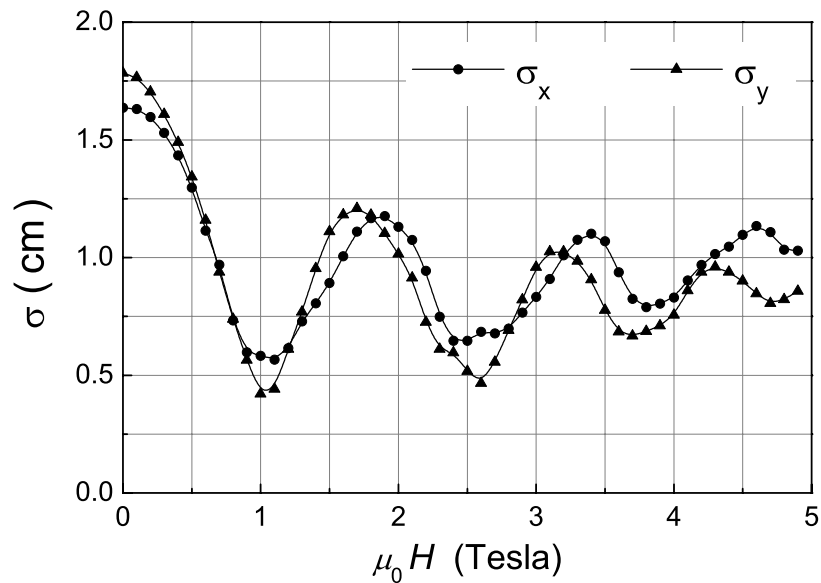


Figure 3: Muon beam spot size (represented by the standard deviations  $\sigma_{x,y}$  for the two distributions along the X and Y directions) measured with the  $\mu$ BPM in the center of the ALC solenoid as a function of the applied magnetic field  $H$ .

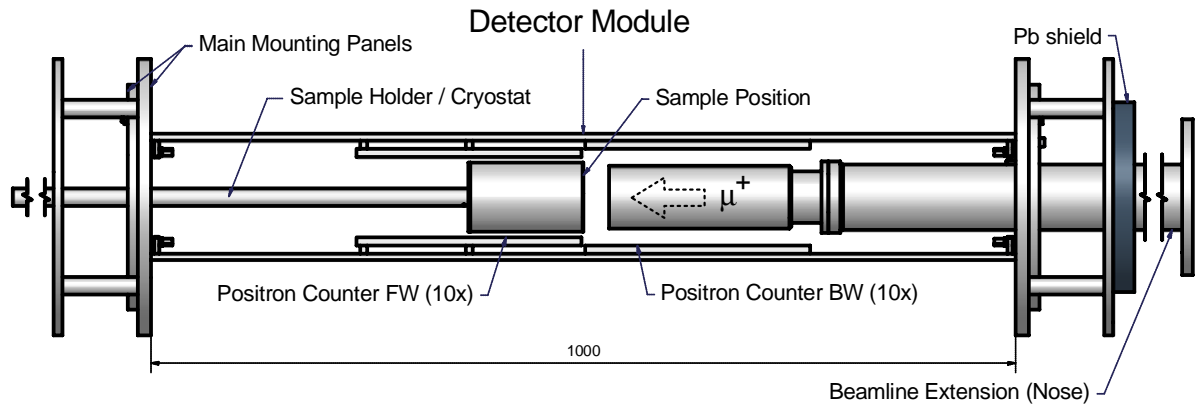


Figure 4: ALC spectrometer: mounting of the detector module in the warm bore of the solenoid (the solenoid is not shown).

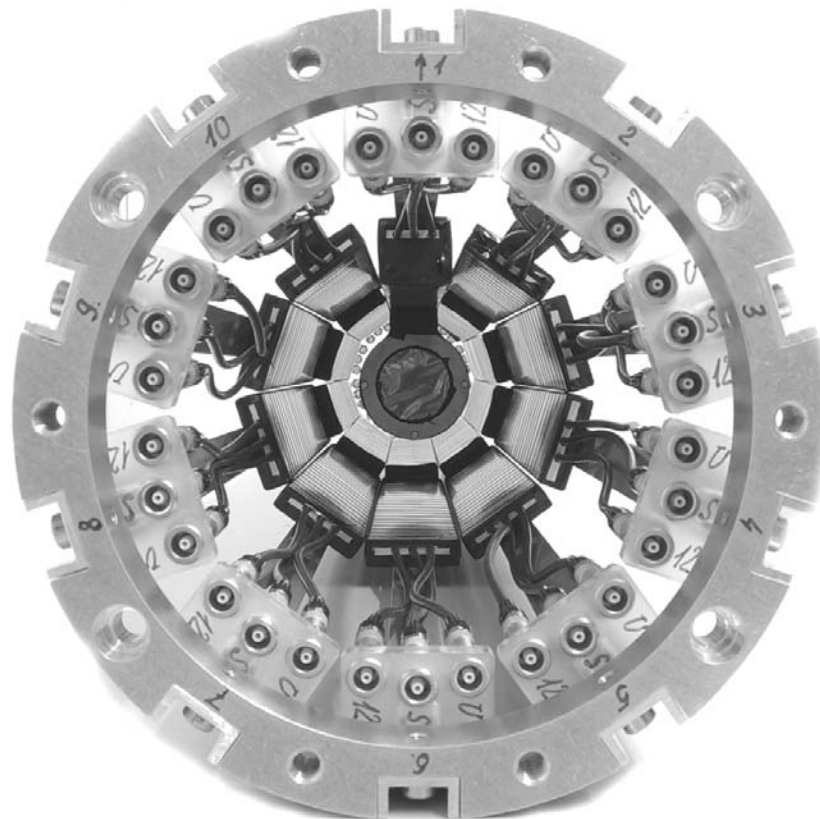


Figure 5: ALC spectrometer: detector module in assembly. View along the direction of the muon beam. One of the positron counters is replaced by a muon counter for the time differential mode of operation.

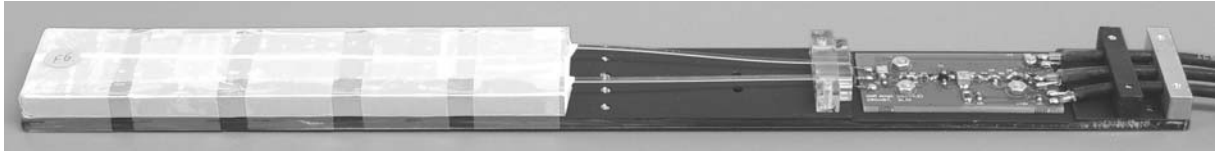


Figure 6: ALC spectrometer: positron counter. The lid for mechanical protection and the black tape wrapping for light protection have been removed.

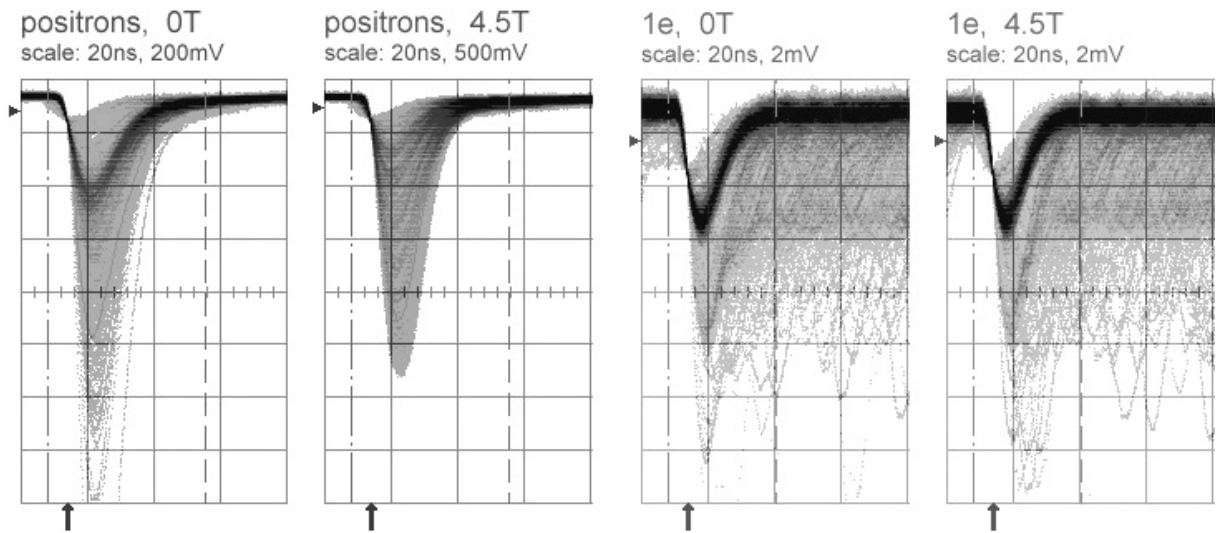


Figure 7: ALC spectrometer: detection of positrons in one of the counters and its  $1e^-$ -signals (the signals initiated by thermally generated charge carriers) both in presence of 4.5 T magnetic field and in zero field. Note the different vertical scales.

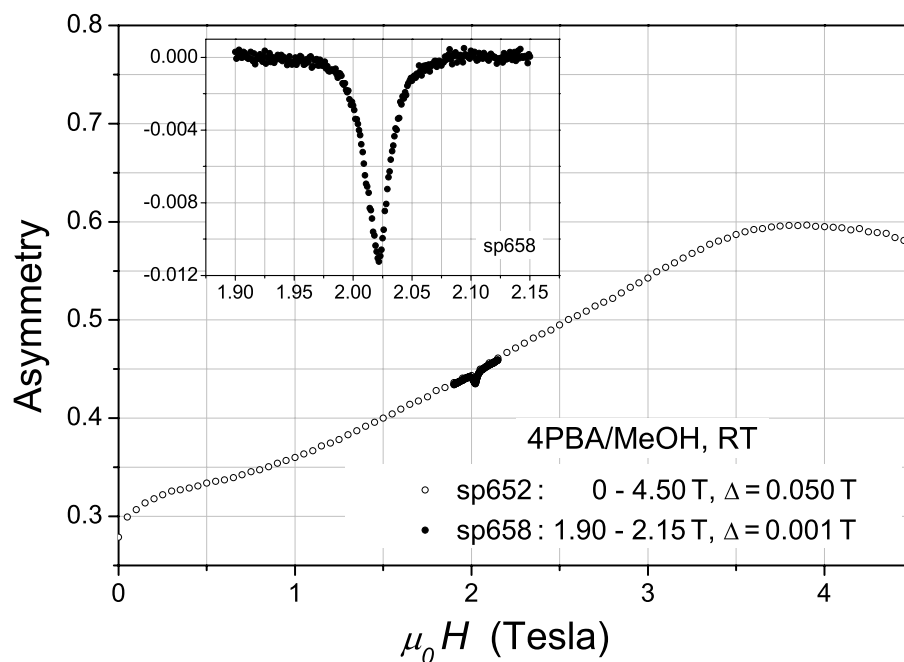


Figure 8: ALC spectra taken on a 4PBA/MeOH (4-propyl-benzoate / methanol) sample at room temperature: a wide field range scan (sp652) and a short range scan (sp658) over the resonance at around 2 T. The insert shows sp658 after the subtraction of a straight baseline.

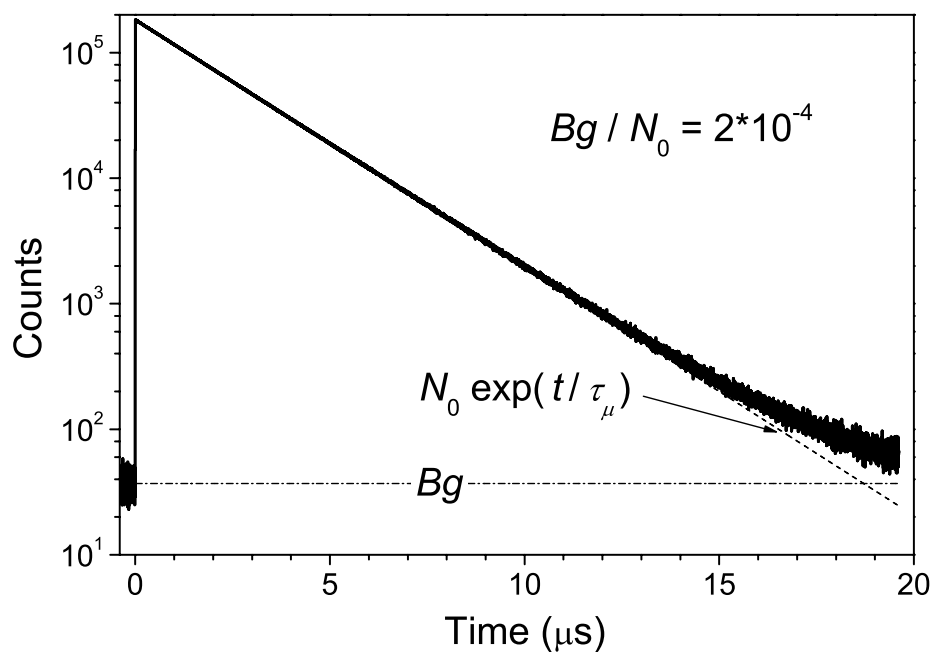


Figure 9: Time-differential  $\mu$ SR spectrum taken with the new ALC detector on a silver sample in zero magnetic field.

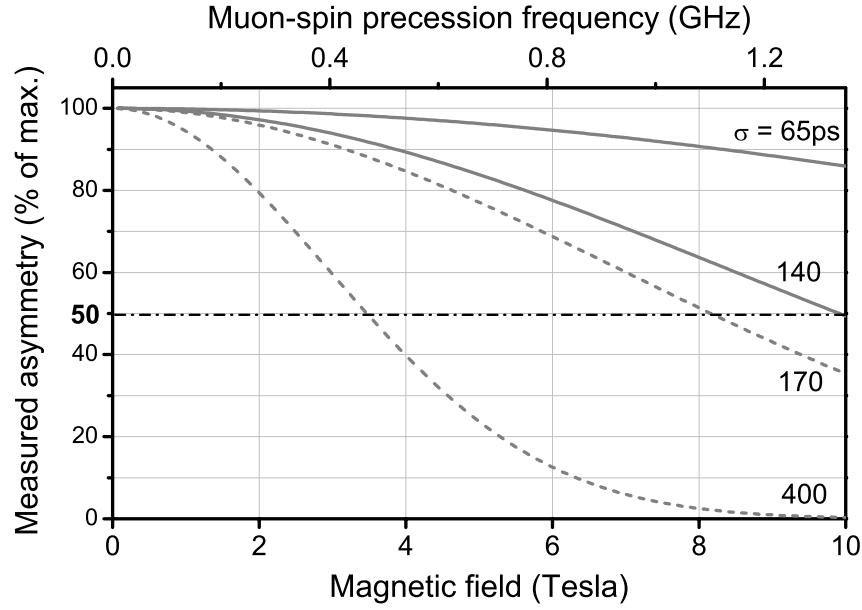


Figure 10: Decrease of the measured amplitude of the muon-spin precession signal with increasing its frequency (magnetic field) for different values of the spectrometer time resolution: 400 ps – characteristic time resolution of a “standard”  $\mu$ SR spectrometer; 170 ps – 7 Tesla *HiTime* instrument at TRIUMF; 140 ps – upper limit for a 10 T spectrometer; 65 ps – time resolution demonstrated with G-APD based prototype detectors.

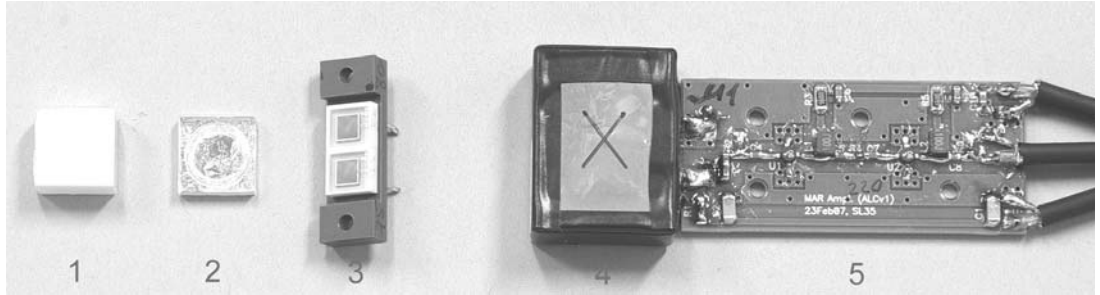


Figure 11: Fast-timing muon and positron counters (prototypes): 1) 10 x 10 x 5 mm EJ-232 (Eljen Technology) plastic scintillator wrapped in Teflon tape; 2)  $\varnothing 8 \times 0.3$  mm EJ-232 scintillator glued into a 10 x 10 x 2 mm frame with  $\varnothing 7$  mm central hole made of BC-800 (Saint-Gobain Crystals) plastic. 7  $\mu$ m thick aluminized Mylar foil is used as a reflector; 3) two G-APDs of type MPPC S10362-33-050 (Hamamatsu Photonics) connected in series (the bias voltage for the pair is  $\sim 140$  V, the operating point is chosen at a dark current value of  $I_0 = 4.0 \mu\text{A}$ ); 4) light tight box containing a scintillator (1) or (2) coupled to the photosensor (3). Optical contact is ensured by using optical grease BC-630. The windows of the box are made of 10  $\mu$ m thick Ti-foil; 5) broad band amplifier (gain  $\sim 13$ , bandwidth  $\sim 600$  MHz).

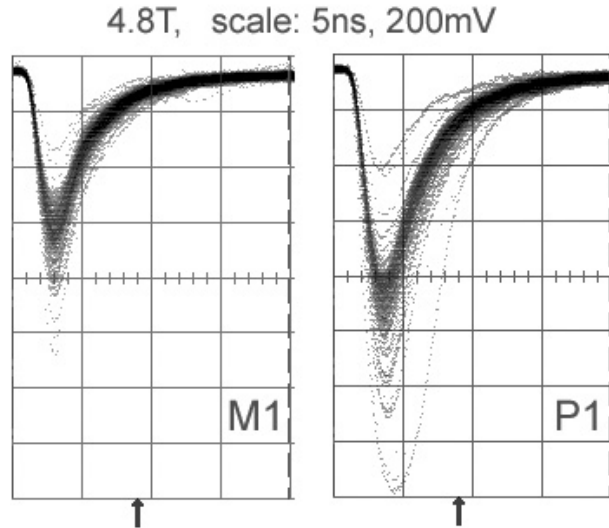


Figure 12: Fast-timing counters: detection of 28 MeV/c muons (M1) and positrons (P1) in 4.8 T magnetic field. The detection thresholds are set at 230 mV. The averaged rise / fall times of the signals are: M1 – 1.24 / 7.2ns, P1 – 1.48 / 8.0ns.

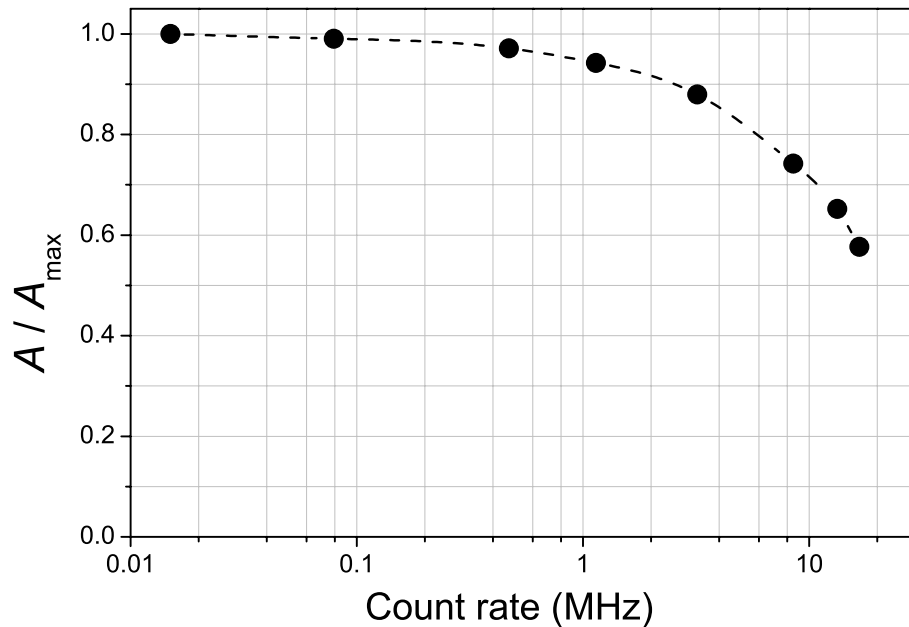


Figure 13: Fast-timing positron counter: rate dependence of the most probable signal amplitude. The measurement was done in a 4.8 T field, the positron beam intensity was varied by the beamline slit system. The dashed line is drawn to guide the eye. The decrease of the amplitude with increasing rate is due to the finite recovery time of the G-APD.